A computer model of amplitude-modulation sensitivity of single units in the inferior colliculus

Michael J. Hewitt and Ray Meddis
Speech and Hearing Laboratory, Department of Human Sciences, University of Technology, Loughborough LE11 3TU, United Kingdom

(Received 20 July 1993; accepted for publication 8 December 1993)

A computer model is presented of a neural circuit that replicates amplitude-modulation (AM) sensitivity of cells in the central nucleus of the inferior colliculus (ICC). The ICC cell is modeled as a point neuron whose input consists of spike trains from a number of simulated ventral cochlear nucleus (VCN) chopper cells. Input to the VCN chopper cells is provided by simulated spike trains from a model of the auditory periphery [Hewitt *et al.*, J. Acoust. Soc. Am. **91**, 2096–2109 (1992)]. The performance of the model at the output of the auditory nerve, the cochlear nucleus and ICC simulations in response to amplitude-modulated stimuli is described. The results are presented in terms of both *temporal* and *rate* modulation transfer functions (MTFs) and compared with data from physiological studies in the literature. Qualitative matches were obtained to the following main empirical findings: (a) Auditory nerve temporal-MTFs are low pass, (b) VCN chopper temporal-MTFs are low pass at low signal levels and bandpass at moderate and high signal levels, (c) ICC unit temporal-MTFs are low pass at low signal levels and broadly tuned bandpass at moderate and high signal levels, and (d) ICC unit rate-MTFs are sharply tuned bandpass at low and moderate signal levels and flat at high levels. VCN and ICC units preferentially sensitive to different rates of modulation are presented. The model supports the hypothesis that cells in the ICC decode temporal information into a rate code [Langner and Schreiner, J. Neurophysiol. **60**, 1799–1822 (1988)], and provides a candidate wiring diagram of how this may be achieved.

PACS numbers: 43.64.Qh, 43.64.Bt

INTRODUCTION

The inferior colliculus (IC) has been described as the nexus of the mammalian auditory system (Aitkin, 1986). The nucleus receives input from numerous brain-stem nuclei and, in turn, tonotopically projects neurons towards the auditory cortex via the medial geniculate body of the thalamus. It is thought that IC processing is performed within highly parallel streams, where each stream codes a perceptually relevant feature of a complex sound source.

One common feature of many complex and natural sounds is the repetition rate of amplitude fluctuations. Periodic amplitude modulations characterize voiced speech sounds and engender the perception of pitch. The pitch of a sound source is a powerful cue in helping us to attend to one speaker in the presence of other, competing voices (e.g., Assmann and Summerfield, 1989). In this paper we address the role of certain cells in the central nucleus of the inferior colliculus (ICC) that are preferentially sensitive to particular rates of amplitude modulation (AM).

It has been hypothesized that cells in the ICC form part of a neural periodicity detection system (Langner and Schreiner, 1988; Langner, 1992). The theory is based on physiological data which suggest that the ICC has a perio-dotopic organization which lies roughly orthogonal to its tonotopic axis. The temporal selectivity along the perio-dotopic axis is most strongly represented by a rate code. Examples of this temporal selectivity are reproduced in Fig. 1 which shows the responses of cat ICC neurons to a range of amplitude-modulated tones. Similar data have been presented for rat and guinea pig ICC units by Rees and his colleagues (Rees and Møller, 1983; Rees and Palmer, 1989).

Neuronal responses at the lower levels of the ascending auditory system appear only to represent signal periodicity by a temporally based (phase-locked) code. For example, ventral cochlear nucleus chopper cells selectively amplify signal modulation and show sharply tuned bandpass temporal modulation transfer functions, but the selectivity is not manifest in a rate representation (Frisina *et al.*, 1990; Kim *et al.*, 1990). It is likely that the transformation from a temporal-based periodicity code to a rate-based one first occurs within the ICC. Given that neural synchronization at higher levels of the auditory system is poor (Rees and Møller, 1983; Eggermont, 1991), then this process may be considered as crucial if information about signal periodicity is to be passed to higher auditory centers.

The purpose of this paper is to present and evaluate a computer model of a neural circuit that transforms a temporal-based periodicity code in to a rate-based one. The circuit we propose comprises an ICC unit that receives input from many cochlear nucleus chopper cells which, in turn, receive input from many auditory-nerve fibers. The cochlear nucleus units serve to selectively enhance periodicities present in the signal. At this stage the output spike rate is the same for all AM rates; it is only the pattern of timing of the spikes which changes. We speculate that the ICC unit functions as a coincidence detector taking input

 0001-4966/94/95(4)/2145/15/$6.00

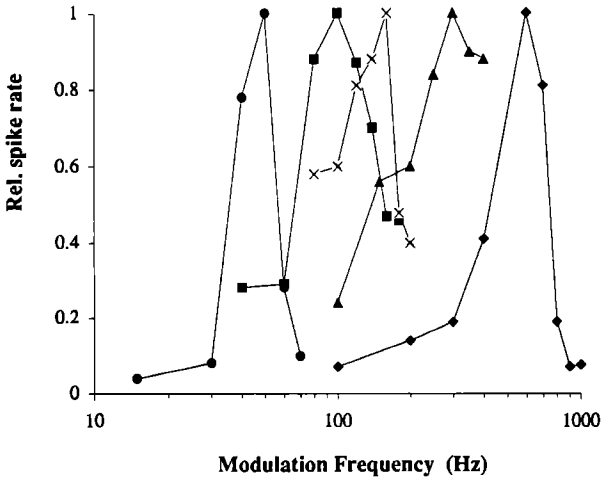

FIG. 1. Normalized rate modulation transfer functions (rate-MTFs) of typical bandpass units of cat ICC. Redrawn from Langner and Schreiner (1988, Fig. 3).

from a number of similar cochlear nucleus chopper cells. The coincidence unit fires only when it receives a number of synchronous cochlear nucleus inputs. The circuit is sufficient to encode signal periodicity as a rate-based code.

The implementation of the circuit builds upon previous modeling studies that described AM-sensitivity in ventral cochlear nucleus chopper units (Hewitt *et al.*, 1992). The chopper model was based on a simplified model of spike generation preceded by a stage that simulated dendritic low-pass filtering. Input to the model was in the form of simulated auditory-nerve spikes produced by a model of the auditory periphery. In the work reported here, we have modeled an ICC unit using the same chopper model as previously described but with parameter changes. Input to the model ICC unit is taken from a number of simulated cochlear nucleus chopper cells all of which have the same intrinsic membrane properties.

We show that the model ICC unit has a number of emergent response properties which are characteristic of neural AM-sensitive units. Model data are quantified and compared to neural data collected by Rees and his colleagues (Rees and Møller, 1983, 1987; Rees and Palmer, 1989) and Langner and Schreiner (1988). Additionally, model data collected from the auditory nerve and cochlear nucleus simulations are presented and compared to corresponding neural data from the literature.

I. METHODS

A. Model description

The model comprises four main stages. A diagrammatic representation of the model is shown in Fig. 2. The first two stages represent cochlear filtering and inner-hair cell transduction of the peripheral auditory system. The third stage models the chopper cells of the ventral cochlear nucleus. These stages have been described in previous publications (e.g., Meddis and Hewitt, 1991; Hewitt *et al.*, 1992), but are briefly summarized below.

1. Cochlear mechanical filtering

Simulation of the mechanical filtering action and frequency selectivity of the basilar membrane was achieved using a single, linear, bandpass, digital filter based on the gamma-tone function (Patterson *et al.*, 1988). The required filter is specified by its center frequency. Unless stated otherwise, the center frequency of the filter was 5 kHz. The 3-dB bandwidth of the 5-kHz filter is 577 Hz. Figure 3 shows the output of a gamma-tone filter ("filtered

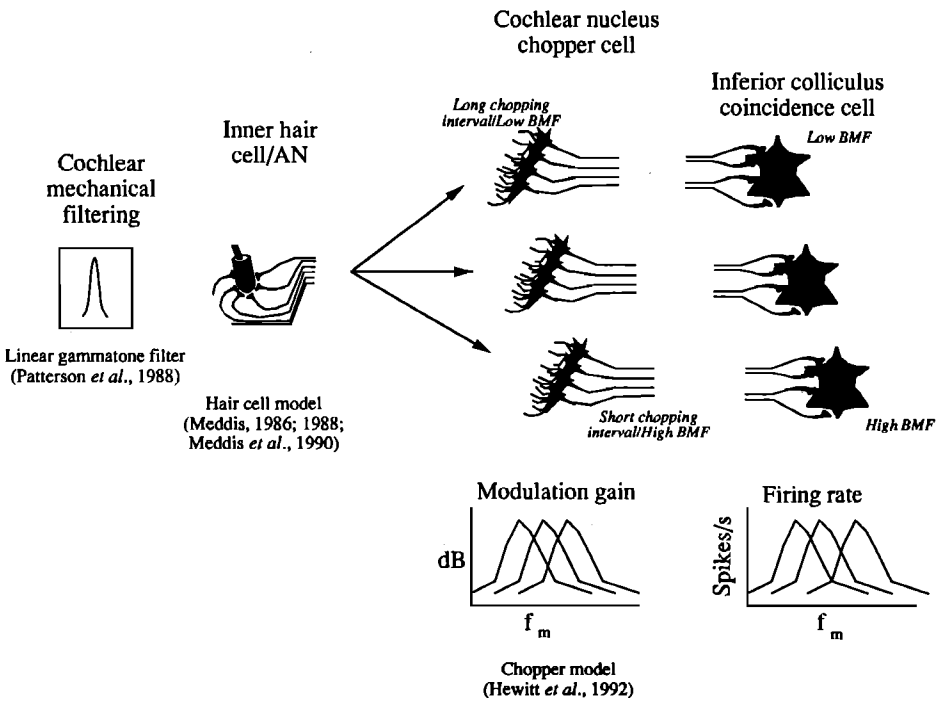

FIG. 2. Diagrammatic representation of the four stage model (see text for details).

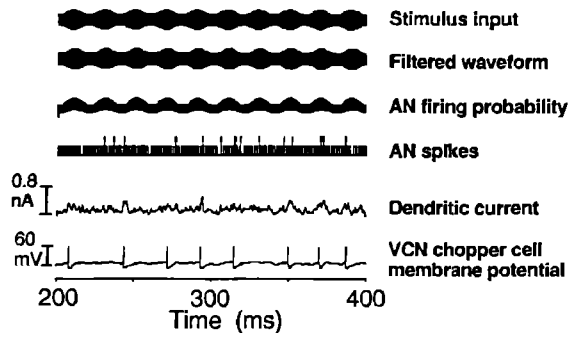

FIG. 3. Model output in response to a pure tone amplitude modulated at 50 Hz, carrier frequency: 5 kHz, 35% AM, input level 30 dB above threshold. The last 200 ms of a 400-ms signal are shown. The AN firing probability represents the output of the Meddis hair cell model. "AN spikes" represents the instantaneous summation of all inputs (max=60) to the cell. The input to the cell is low-pass filtered to simulate dendritic processing, before being passed to the model soma.

waveform") centered on 5 kHz in response to a 5-kHz tone 35% modulated at 50 Hz. In this example, the sideband frequencies of the AM stimulus are within the passband of the filter. At higher modulation frequencies the energy of the sideband components will increasingly move outside the passband of the filter. This leads to a reduction in the synchrony of auditory-nerve firing to the signal's modulation frequency (see Sec. II A).

2. Inner-hair cell/auditory nerve

Simulation of the mechanical to neural transduction process at the inner hair cell/auditory nerve synapse was implemented using the computer model proposed by Meddis (1986, 1988; Meddis *et al.*, 1990). The output of the hair cell is expressed as the probability of occurrence of a spike in an auditory-nerve (AN) fiber of the 5-kHz channel ("AN firing probability," Fig. 3).

The parameters of the hair-cell model were set to simulate a fiber with a spontaneous rate of about 35 spikes/s, a saturated rate of about 150 spikes/s and a limited (30 dB) dynamic range (Hewitt *et al.*, 1992).

Refractory suppression of firing of the auditory nerve was computed as an adjustment to the hair cell firing probability as a function of time since it last generated a spike (see Meddis and Hewitt, 1991 for details). Individual AN spikes were generated from the hair-cell firing probability using pseudorandom number techniques (e.g., Hastings and Peacock, 1975, p. 41). Due to the probabilistic nature of the technique, a different pattern of auditory-nerve spikes is generated with each stimulus presentation. Unless stated otherwise, 60 auditory-nerve fiber inputs, all with the same center frequency, were simulated. The output of this stage represents the number of active (spiking) auditory-nerve fibers per time unit simulated ("AN spikes," Fig. 3), and forms the input to the ventral cochlear nucleus chopper model.

3. Ventral cochlear nucleus chopper cell

The sustained-chopper units of the ventral cochlear nucleus were implemented exactly as described in our earlier work (Hewitt *et al.*, 1992). The initial development of the model was constrained by the known anatomy of VCN stellate cells. Such cells generally show a chopper poststimulus time histogram response pattern to characteristic-frequency (CF) pure-tone stimulation (e.g., Smith and Rhode, 1989).

The model comprises two stages. First, the train of incoming auditory-nerve spikes is low-pass filtered to simulate dendritic filtering of the cochlear nucleus stellate cells. The filter was implemented as a first-order low-pass digital filter to give 6-dB attenuation per octave. The main consequence of low-pass filtering is that the auditory-nerve input is smeared over time. The effects of a spike are not simply instantaneous, but continue to influence the cell membrane for some time after ("dendritic current," Fig. 3). Such effects are observed empirically (e.g., Oertel, 1985; Oertel *et al.*, 1988).

The second stage of the chopper model simulates spike generation at stellate cell somata. This was achieved using a simplified model of the Hodgkin and Huxley (1952) equations of spike generation (MacGregor, 1987). The model has a number of properties characteristic of VCN stellate cell somata including a linear current/voltage curve (Hewitt *et al.*, 1992). The differential equations describing the model are presented in the Appendix. Figure 3 shows the time-varying cell membrane potential of a model unit in response to a CF tone modulated at 50 Hz.

4. ICC model

The novel aspect of the research reported here concerns processing at the ICC level. In the simulations reported below, the output spikes of a number of VCN chopper cells formed the input to a single ICC unit. The model chopper cells all had the same parameters, but their outputs differed because of the stochastic nature of their auditory-nerve inputs. The ICC unit was modeled by the same two-stage simulation used for the VCN chopper cell but with parameter changes. These changes are indicated in the Appendix (Table AI) and represent a neuron with a relatively high threshold with relatively fast time constants of prespike integration and postspike recovery. Examples of output from this stage of the model are presented later in the paper (Fig. 18).

We have previously used the VCN chopper model to replicate the preferential sensitivity of chopper units to different rates of amplitude modulation (Hewitt *et al.*, 1992). The sensitivity is manifest in an increase in the synchrony of the timing of spike output to the peaks of the amplitude envelope of the driving signal. Such output may be quantified using the modulation gain metric (defined below). When modulation gain is plotted as a function of modulation frequency, a bandpass function often results. The frequency at which the peak modulation gain is found is commonly referred to as the best-modulation frequency (BMF). The work showed that the BMF of a given unit was equal to the reciprocal of the unit's interspike interval. The interspike interval could be manipulated by changing a single parameter of the chopper cell soma model (τ_{Gk}, the time constant of potassium conductance). Hence it is

possible to create a number of neurons each with different interspike intervals and consequently different best-modulation frequencies. This arrangement is shown diagrammatically in Fig. 2. Each population of chopper cells feeds a single model ICC cell. The output of each model ICC cell displays a rate sensitivity to amplitude modulation; the frequency of maximum response is governed by the BMF of the input chopper cells. Examples of model VCN chopper and ICC units with different BMFs are presented in Sec. II of the paper.

B. Analysis of model output

The physiological study of neural responses to periodic stimuli is often expressed using modulation transfer functions (MTFs). These are defined as the amount of neural activity evoked by amplitude-modulated best-frequency tones as a function of modulation frequency.

The amount of neural activity can be quantified in different ways. First, it can be expressed as a neuron's firing rate. Second, a period histogram can be constructed and the *degree of synchrony* of the evoked activity to the stimulus envelope can be measured using the vector strength metric (Goldberg and Brown, 1969). Vector strength (r) is calculated as

$$r=\frac{\sqrt{[\Sigma_0^{K-1}R_k\cos 2\pi(k/K)]^2+[\Sigma_0^{K-1}R_k\sin 2\pi(k/K)]^2}}{\Sigma_0^{K-1}R_k}, \quad (1)$$

where K=the number of bins in the period histogram, and R_k=the magnitude of the kth bin.

A third metric may also be used which combines both rate and synchrony information. This involves measuring the magnitude of the Fourier component at the modulation frequency and gives the neural firing rate (in spikes/s) synchronized to the modulation waveform. This can be calculated directly using the expression $2rm$ where r is the vector strength [Eq. (1)] and m is the mean firing rate to the modulated stimulus.

Using these different metrics three types of MTF can be constructed. First, the rate-MTF which shows the firing rate of a neuron at a given signal level plotted as a function of modulation frequency. Second, the temporal-MTF which shows the modulation gain of a neuron at a given signal level plotted as a function of modulation frequency. Modulation gain (in dB) is calculated as follows:

$$\text{modulation gain}=20\log_{10}(200r/\%\text{modulation depth of the stimulus}), \quad (2)$$

where r=the vector strength [Eq. (1)] of the response period histogram.

Finally the third metric, which combines both rate and synchrony information (i.e., the magnitude of the modulation-frequency response component), can be plotted as a function of modulation frequency. Following the terminology of Rees and Palmer (1989) this will be referred to as the modulation-frequency magnitude function (MFMF).

Pure-tone stimuli 35% (or 50%) amplitude modulated were used. The frequency of modulation varied between 5 and 1000 Hz. The duration of the stimuli was either 200 or 600 ms. We applied the analysis techniques described above to the output of the model at the level of the auditory nerve, the cochlear nucleus chopper cell, and the ICC unit. Additional analysis of the properties of the ICC unit is presented at the end of the section. All of the results are compared to the corresponding neural data.

All simulations were programmed in FORTRAN 77 on a Masscomp 5450 computer. The step integration size (dt) was 20 μs (50-kHz sample rate).

II. MODEL EVALUATION

A. Auditory nerve

A number of investigators have studied the responses of single auditory-nerve fibers to sinusoidally amplitude modulated tones (e.g., Møller, 1976; Javel, 1980; Palmer, 1982; Frisina *et al.*, 1990; Kim *et al.*, 1990; Khanna and Teich, 1989; Joris and Yin, 1992). For a given signal level the average firing rate of auditory-nerve fibers appears to be independent of modulation frequency. In contrast, the degree of synchronization varies with modulation frequency. Typical temporal modulation transfer functions are low-pass in shape with cutoff frequencies below 1 kHz (dependent on CF of fiber, see Palmer, 1982). Some deviations from this pattern are observed at high signal levels where a rudimentary peak (also below 1 kHz) may exist in the transfer function (Kim *et al.*, 1990).

Figure 4 shows AN data from the study of Joris and Yin (1992) together with data from the output of the AN model used in this study. The main qualitative aspects of the neural data, namely a flat rate-MTF and a low-pass temporal-MTF, are replicated by the model. The decrease in the phase-locked response at AM frequencies above 1 kHz is attributed to the movement of the energy of the stimulus sidebands out of the response area of the fiber as the modulation frequency is increased (Javel, 1980; Palmer, 1982).

B. Cochlear nucleus

1. Single-unit tuning to amplitude modulation

Following the pioneering work of Møller (1972, 1973, 1976) other investigators have shown that the amplitude-modulation characteristics of a signal are enhanced by certain cells in the cochlear nucleus (Frisina *et al.*, 1990; Kim *et al.*, 1990).

Frisina *et al.* (1990) examined the enhancement of responses to amplitude modulation in single neurons of the gerbil ventral cochlear nucleus. The majority of units in Frisina's study were classified as sustained chopper units. To quantify the enhancement of amplitude modulation, Frisina calculated the modulation gain for each neuron in response to characteristic-frequency tones amplitude modulated over a range of low frequencies (25–1000 Hz).

Temporal modulation transfer functions are low pass for stimulus levels below about 20 dB (*re*: threshold) and narrowly tuned bandpass functions for levels above this

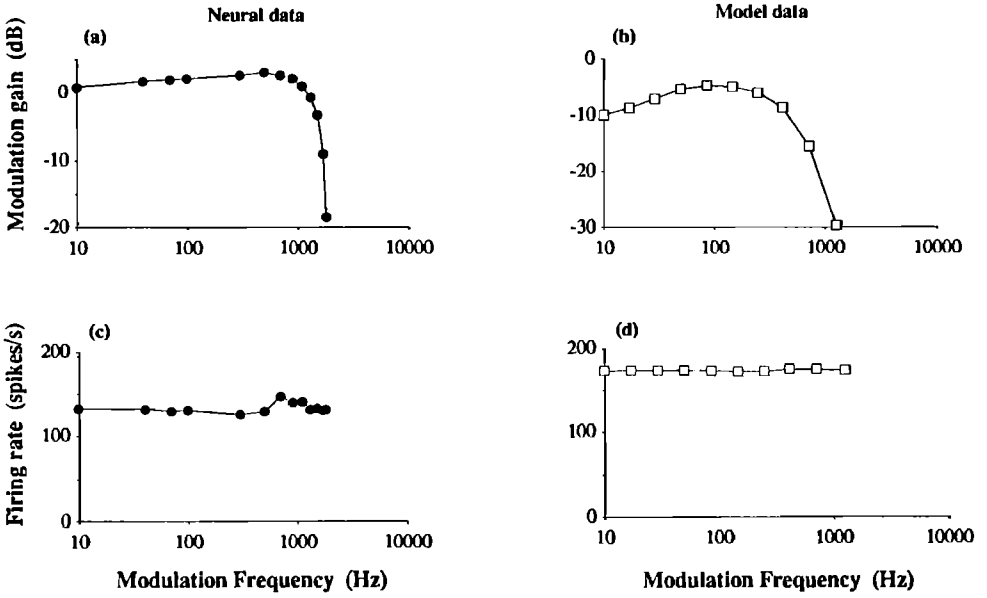

FIG. 4. Temporal and rate modulation transfer functions. (a) and (c) from AN fiber recordings (redrawn from Joris and Yin, 1992, Fig. 10). CF of fiber=21 kHz. (b) and (d) from AN model. Stimulus level 20 dB above threshold.

[Fig. 5(a), redrawn from Frisina *et al.*, 1990, Fig. 12, unit 131]. Frisina *et al.* (1990) noted that the peak-modulation gain was maximal at 30 dB then decreased on average by about 5 dB for stimulus-input levels between 30 and 50 dB.

Figure 5(b) shows MTFs derived from chopper-cell model responses to a 5-kHz tone which was amplitude modulated over a range of frequencies for three different input levels. The model replicates the main qualitative features of the neural temporal MTFs, namely; a low-pass function at low stimulus levels, bandpass functions at moderate and high stimulus levels, and a reduction in the peak modulation gain as input level increases.

Kim and his colleagues (Kim *et al.*, 1990) presented temporal-MTFs, rate-MTFs and modulation-frequency magnitude functions (response to $f0$ as a function of modulation frequency) from chopper neurons located in the PVCN and DCN of cat. They found that neurons with bandpass temporal-MTFs (as above) had flat rate-MTFs, and bandpass modulation-frequency magnitude functions [see Fig. 6(a)].

Figure 6(b) shows that the model's response component to the fundamental frequency of the stimulus varied systematically with modulation frequency in a manner consistent with the neural data. The average response rate is independent of modulation frequency also in accordance with neural data. That is, in common with the neural data the model achieves an enhancement of modulation by an increase in the synchronization of firing to the $f0$ component of the stimulus.

Further details and discussion of the properties of the cochlear nucleus chopper cell model are documented in Hewitt *et al.* (1992) and Hewitt and Meddis (1993). Other models of cochlear nucleus cells are presented by Arle and Kim (1991) and Banks and Sachs (1991). Ghoshal *et al.* (1992) have also presented a model of the AM encoding properties of cochlear nucleus cells.

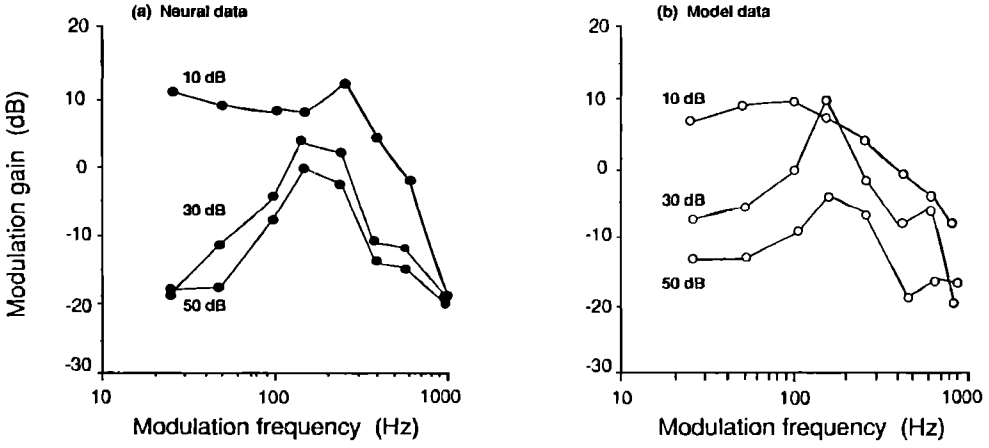

FIG. 5. VCN chopper temporal modulation transfer functions. Parameter: input level above threshold. (a) Neural data redrawn from Frisina *et al.*, 1990 (top panel, Fig. 12). (b) Model data. Model parameters: 200-ms duration, AM-signals, 35% AM, stimulus repetitions: 40 per datum, τ_{Gk}: 1 ms.

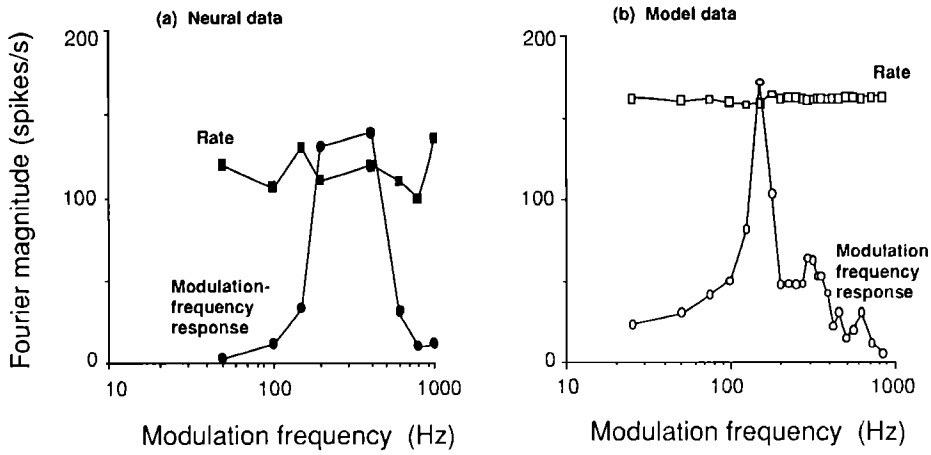

FIG. 6. VCN chopper rate modulation transfer functions (squares) and modulation-frequency magnitude functions (circles). (a) Neural data from Kim *et al.* (1990, bottom panel, Fig. 2). (b) Model parameters: stimulus input level 30 dB, 35% AM, 200-ms duration, stimulus repetitions: 40 per datum.

2. Modeling populations of VCN chopper cells

Physiological studies of cochlear nucleus chopper cells (e.g., Frisina *et al.*, 1990; Kim *et al.*, 1990) suggest that for each characteristic frequency there exists an array of neurons which are systematically tuned to different rates of amplitude modulation. The sensitivity to modulation rate across the array ranges from about 50 to 400 Hz.

The sensitivity to modulation rate by the model chopper cell used in this and a previous study (Hewitt *et al.*, 1992) can be manipulated by changing certain parameters of the point-neuron model (MacGregor, 1987). The parameter τ_{Gk} (the time constant of potassium conductance) is particularly useful in this respect. In the case of Fig. 5 above, where τ_{Gk} was set at 1.0 ms, the peak modulation gain was at about 150 Hz.

Figure 7 shows the best modulation frequency (*re*: 30 dB above threshold) of the model as a function of τ_{Gk}. The parameter τ_m (the membrane time constant) also influenced the best modulation frequency of the model. The combined effect on model best modulation frequency for different values of τ_m and τ_{Gk} is also shown in Fig. 7. The figure demonstrates that a suitable range (e.g., 50–400 Hz) of best modulation frequencies can be generated by the model.[1]

Figure 8 shows bandpass temporal modulation transfer functions of three model units (BMFs of 100, 200, and 400 Hz) all with a characteristic frequency of 5 kHz. These will be referred to in Sec. II C 2 below.

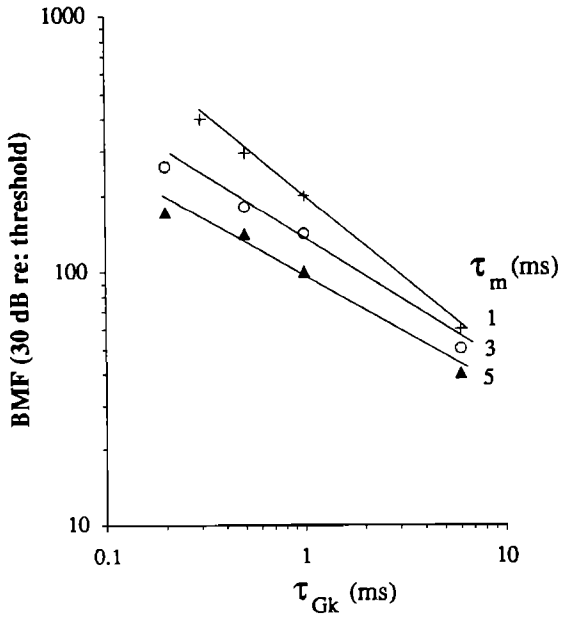

FIG. 7. Position of model VCN chopper best-modulation frequency as a function of model parameter τ_{Gk} and for different values of τ_m. (Straight lines fitted by eye.)

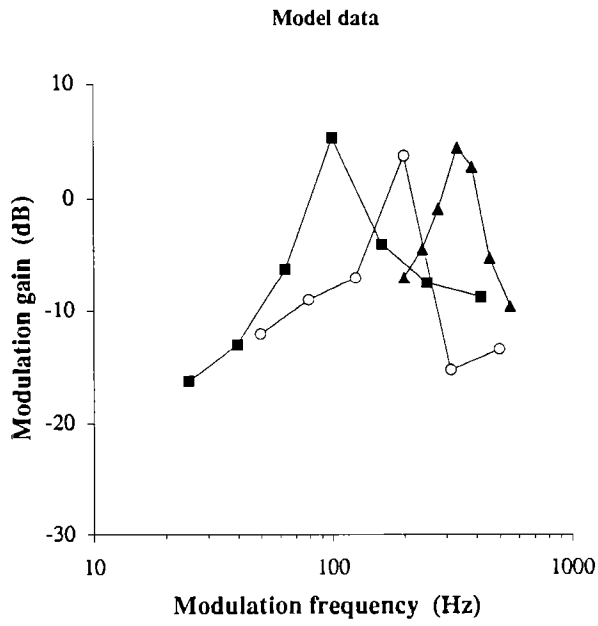

FIG. 8. VCN chopper temporal modulation transfer functions. Model parameters: 200-ms duration, AM signals, 50% AM, 30 dB above threshold, 20 stimulus repetitions per datum. Filled squares: BMF=100 Hz, τ_{Gk}=3 ms. Open circles: BMF=200 Hz, τ_{Gk}=0.5 ms. Filled triangles: BMF=400 Hz, τ_{Gk}=0.3 ms, τ_m=1 ms.

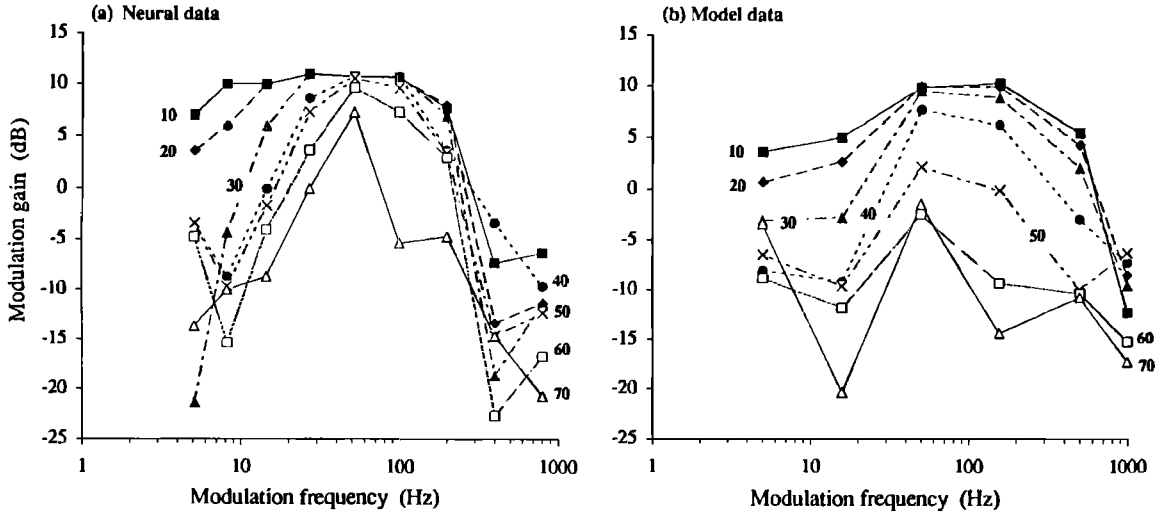

FIG. 9. Temporal MTFs at different stimulus levels. (a) Neural ICC data redrawn from Rees and Palmer (1989, Fig. 4). CF=5.5 kHz. (b) Model data. CF=5.0 kHz, 30 stimulus repetitions per datum, 600-ms duration, 50% AM.

C. Inferior colliculus

1. Single-unit tuning to amplitude modulation

Responses from units in the central nucleus of the inferior colliculus show a bandpass sensitivity to AM rate, i.e., the response is smaller at modulation rates on either side of some best rate. The bandpass sensitivity is manifest in terms of both rate and synchrony measures (Rees and Møller, 1983, 1987; Langner and Schreiner, 1988; Rees and Palmer, 1989). Other studies of AM processing in the mammalian inferior colliculus have been reported by Batra *et al.* (1989), Lesser *et al.* (1990), and Müller-Preuss *et al.* (1988).

One of the most comprehensive studies is that of Rees and Palmer (1989). They studied the temporal response patterns of cells in guinea pig ICC in response to amplitude-modulated signals over a range of stimulus levels. Nearly all (97%) of the 89 units they studied responded with a temporal modulation of their neural discharge at one or more modulation frequencies. Data were presented in the form of temporal and rate modulation transfer functions as well as modulation-frequency magnitude functions (response to $f0$ as a function of modulation frequency).

The model data presented in this section are compared to data from Rees and Palmer's exemplar ICC unit. The unit responded preferentially to modulation frequencies of about 50 Hz. In Sec. II B 1 of this article we qualitatively compared model cochlear nucleus chopper cell data to neural data of Frisina *et al.* (1990). To facilitate comparison with Frisina's cochlear nucleus data, the model was tuned to respond preferentially to a modulation rate of about 150 Hz. To generate model chopper cells with best modulation frequencies of 50 Hz we simply adjusted a single parameter (τ_{Gk}) of the point neuron model as described in Sec. II B 2. The results presented below show that the best modulation frequency of a model ICC unit corresponds to that of the model chopper cells that provide its input. In the simulations reported below, the output of 60

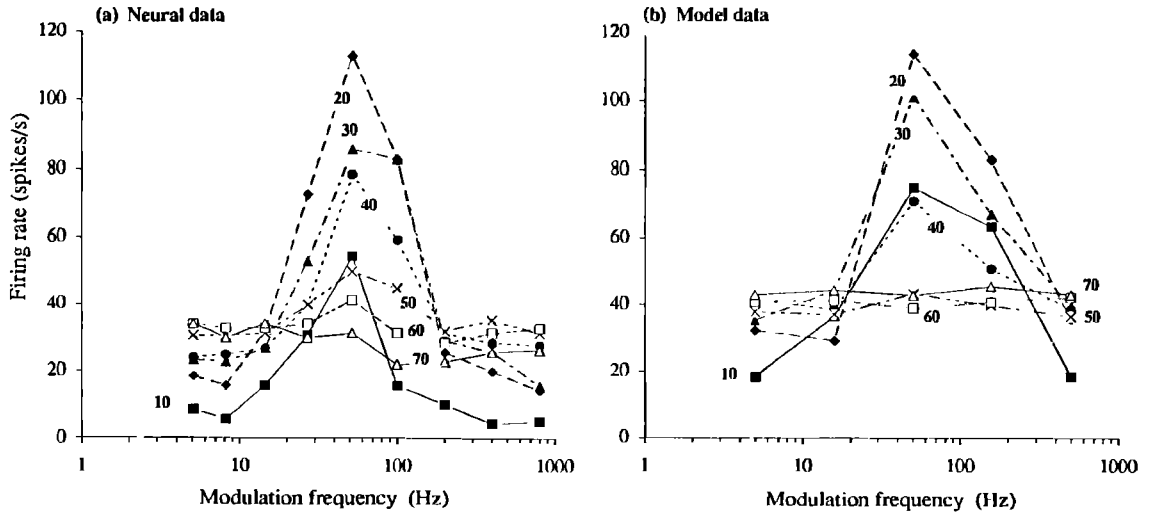

FIG. 10. Rate MTFs at different stimulus levels. (a) Neural ICC data redrawn from Rees and Palmer [1989, Fig. 5(a)]. CF=5.5 kHz. (b) Model data CF=5.0 kHz, 30 stimulus repetitions per datum, 300-ms duration, 50% AM.

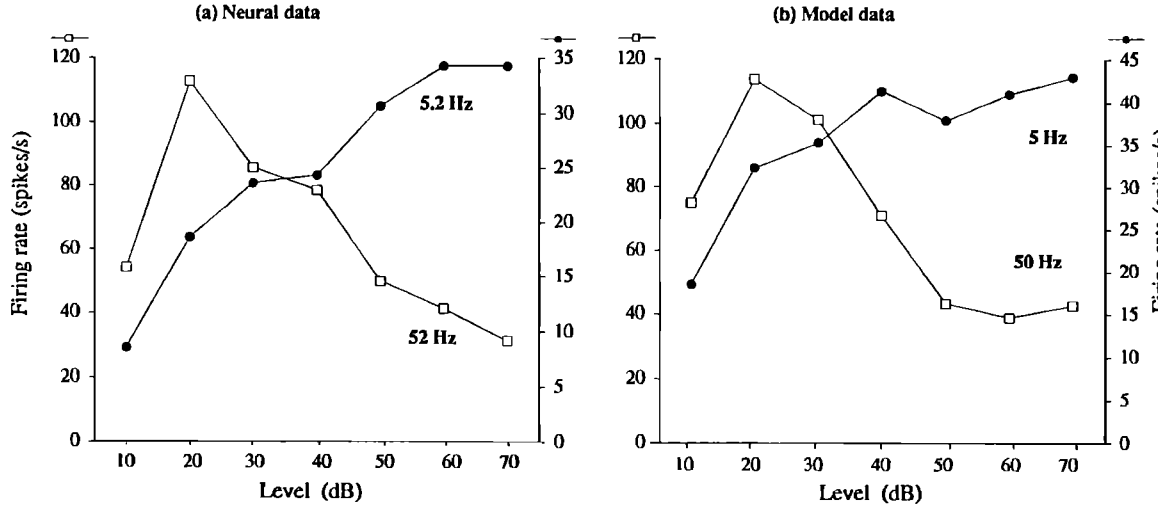

FIG. 11. Mean firing rates to a modulated tone at low modulation frequency (closed circles) and peak modulation frequency (open squares). (a) Neural data from Rees and Palmer [1989, derived from Fig. 5(a)], CF=5.5 kHz. (b) Model data from Fig. 10(b). CF=5.0 kHz.

model VCN chopper cells formed the input to the model ICC unit; the best modulation frequency of the cells is 50 Hz.

(a) Temporal modulation transfer functions. Rees and Palmer (1989) showed that ICC unit temporal-MTFs are signal level dependent. In common with VCN chopper cells, the functions are low pass at low stimulus levels and bandpass at moderate and high stimulus levels. Figure 9 shows model ICC data compared to data from the neural exemplar. The main qualitative features of the neural data are reproduced by the model. One discrepancy concerns the fall in model modulation gain at 50-Hz modulation frequency as signal level increases; between 40 and 70 dB modulation gain falls by about 10 dB. The corresponding neural data fall by only 2–3 dB.

(b) Rate modulation transfer functions. Rate-MTFs collected by Rees and Palmer for the same unit as above are shown in Fig. 10(a). There are a number of aspects to the data. First, for a given signal level the rate response of the cell varies with modulation frequency. The cell fires maximally in response to a tone amplitude modulated at a rate of 52 Hz (for all but the highest signal level used). However, the response to a 52-Hz modulation frequency is a nonmonotonic function of signal level; within 20 dB of the unit's threshold the firing rate increases with increasing signal level, but thereafter decreases with increasing signal level. In contrast, at very low and relatively high modulation frequencies (i.e., <10 Hz and >200 Hz) the firing rate increases with increasing signal level, but saturates at the most intense signal levels used. These relationships are more clearly observable in Fig. 11(a) which shows mean rate responses to tones modulated at 5.2 and 52 Hz as a function of stimulus level.

Model ICC rate-MTFs are shown in Fig. 10(b). The main qualitative features of the neural data are replicated by the model namely, bandpass MTFs and a peak modulation frequency response which has a nonmonotonic dependence on signal level. Additionally, signal levels that

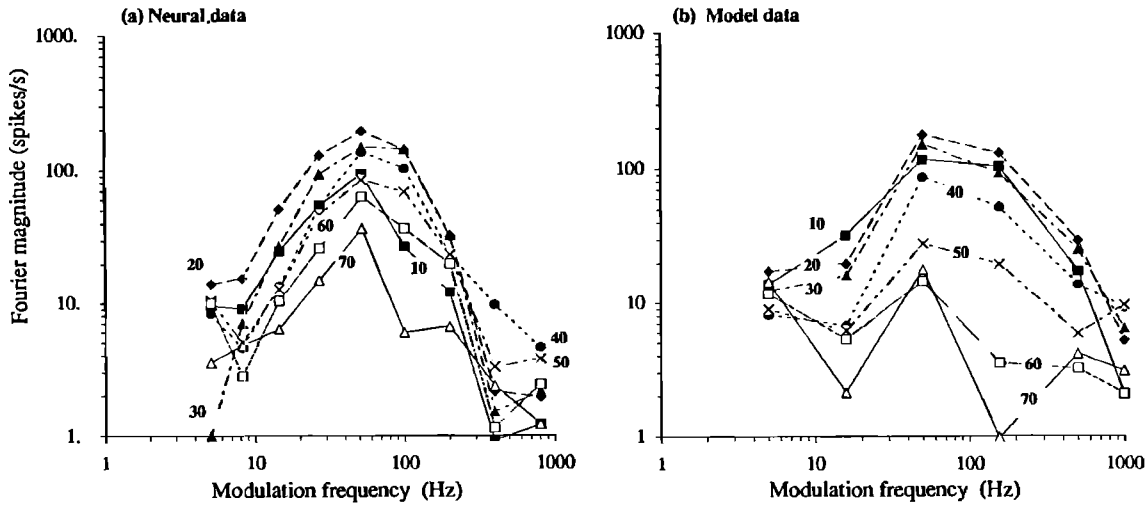

FIG. 12. Modulation frequency magnitude functions at different stimulus levels. (a) Neural ICC data redrawn from Rees and Palmer (1989, Fig. 6). CF=5.5 kHz. (b) Model data. CF=5.0 kHz, 30 stimulus repetitions per datum, 600-ms duration, 50% AM.

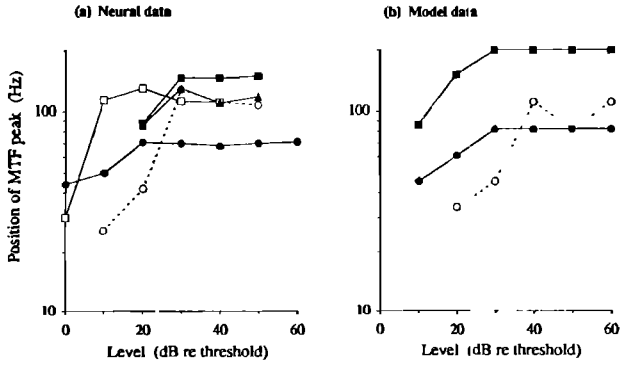

FIG. 13. The influence of stimulus level on the frequency position of the MTF peak. (a) Neural data. Five units from Rees and Moller (1987, Fig. 3). (b) Model data from three units.

give low-pass temporal-MTFs give rise to clear bandpass rate-MTFs.

Figure 11(b) shows model mean rate responses to tones modulated at 5 and 50 Hz as a function of stimulus level. The data compare favorably to the corresponding neural data of Fig. 11(a).

Finally, when comparing the neural temporal-MTFs and rate-MTFs of the same ICC unit two features are notable. First, the peak firing rate of the rate-MTFs occurs at the same modulation frequency that produced the largest modulations gains on the temporal-MTFs. Second, signal levels of 10 and 20 dB above threshold produced bandpass rate-MTFs and low-pass temporal-MTFs. These features are replicated by the model.

(c) Modulation frequency magnitude functions. Rees and Palmer also calculated the magnitude of ICC unit responses to the fundamental frequency of AM stimuli. The metric gives the neural firing rate (in spikes/s) synchronized to the modulation frequency. Data from their exemplar unit are shown in Fig. 12(a) and are compared to model data. The neural functions show similar level and modulation-rate dependencies as the rate-MTFs. However, the functions are more sharply tuned and, in contrast to the rate-MTFs, remain bandpass at the highest signal levels used (60 and 70 dB above threshold). The model functions [Fig. 12(b)] show all of these qualitative features.

(d) Stimulus level. Rees and Møller (1987) noted that the peak response of a neuron's rate modulation transfer function varied with stimulus level. The effect was observed in the majority of the units studied. Typically, the peak shifted to higher modulation frequencies over the first 10–30 dB increase in stimulus level and then showed no further increase with increases in level thereafter [Fig. 13(a)]. This phenomenon was observable in the model ICC rate-MTFs and examples are shown in Fig. 13(b). A similar level-dependent effect has been noted with the temporal-MTFs of cochlear nucleus chopper cells (Kim *et al.*, 1990). The effect was also noted in the model VCN chopper cell [Hewitt *et al.*, 1992, Fig. 8(b)] used in this study, and is the source of the level-dependent changes seen in the rate-MTFs of the model ICC units presented here.

(e) Responses to pure-tone stimuli. Rees and Palmer (1989) measured the pure-tone rate-level function of their exemplar unit. The function increased almost monotonically over a 30-dB range and then saturated. They noted that the function was *qualitatively* similar to the rate-level function derived from the responses to a pure tone modulated at a low frequency (i.e., $\leqslant$10 Hz). This relationship is shown in Fig. 14(a). The same qualitative relationship was found in the model data as shown in Fig. 14(b). The highly nonlinear relationship between stimulus level and firing rate in response to tones modulated at the unit's preferred rate (i.e., 50 Hz, see Fig. 11) is not apparent in the pure tone response. The mechanism that generates these nonintuitive model responses is described in Sec. IV of the paper.

2. Modeling populations of ICC units

On the basis of physiological studies, Langner and Schreiner (1988) have suggested that for each character-

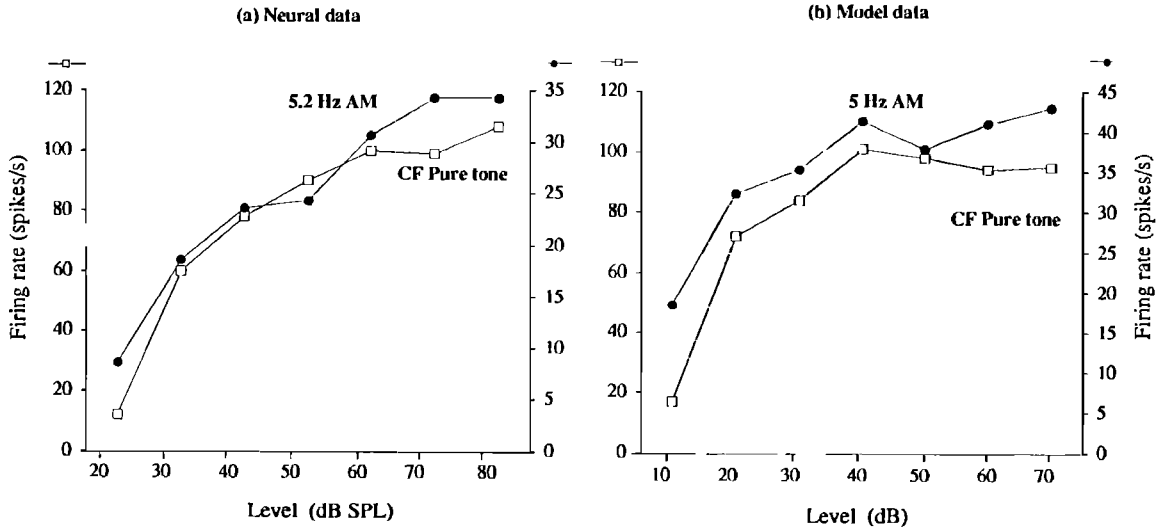

FIG. 14. Mean firing rates to a modulated tone at low-modulation frequency (closed circles) and to an unmodulated CF tone (open squares). (a) Neural data from Rees and Palmer [1989, from Figs. 5(a) and 8(a)], CF=5.5 kHz. (b) Model data, CF=5.0 kHz.

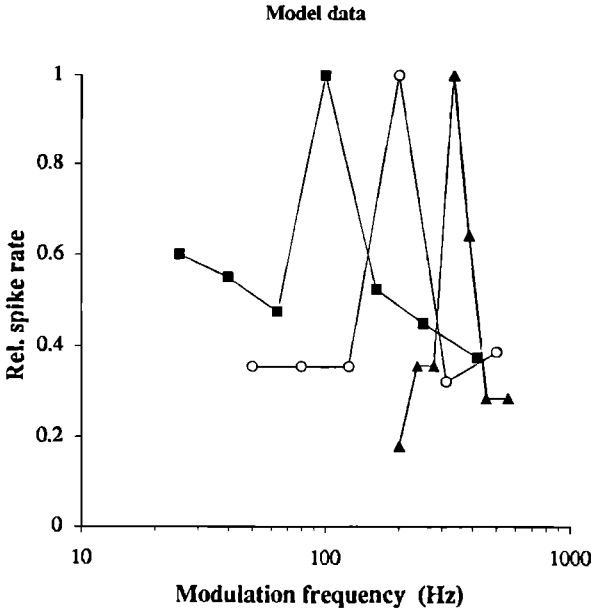

FIG. 15. Model ICC unit rate modulation transfer functions. Stimulus parameters as Fig. 8. Filled squares: BMF=100 Hz, 30 VCN chopper inputs. Open circles: BMF=200 Hz, 18 VCN chopper inputs. Filled triangles: BMF=400 Hz, 11 VCN chopper inputs. Parameters for VCN model chopper units as Fig. 8.

istic frequency there exists an array of neurons sensitive to a range of modulation frequencies. The sensitivity is manifest in the firing rate of individual neurons. The majority of ICC neurons studied by Langner and Schreiner revealed best modulation frequencies between 30 and 100 Hz, other units were preferentially sensitive to higher modulation rates, some as high as 500 Hz.

In Sec. II B 2 above, we modeled populations of VCN chopper cells each with different best modulation frequencies (Fig. 8). The same arrangement can be replicated with the model ICC units. The results are shown in Fig. 15 which shows the output of three model ICC units with peak firing rate responses at 100, 200, and 400 Hz amplitude modulation. The modulation frequency that generates the highest rate response in the model ICC units corresponds to the best-modulation frequency of the VCN chopper cells that provide their input.

III. EFFECTS OF VARYING MODEL PARAMETERS

The number of VCN chopper units innervating each ICC unit influences the model's output. To generate the bandpass rate-MTFs of Fig. 15 we needed to reduce the number of VCN chopper units to each model ICC unit as best-modulation frequency increased. For example, the model ICC unit with a BMF of 100 Hz received input from 30 VCN chopper cells, the unit with a BMF of 200 Hz received 18 inputs and the unit with a BMF with 400 Hz received 11 inputs. In the latter example, the model seemed highly sensitive to a small increase in the number of inputs. The result of "too many" inputs was a loss of preferential sensitivity to 400-Hz modulation shown by a flat rate-MTF [Fig. 16(a)].

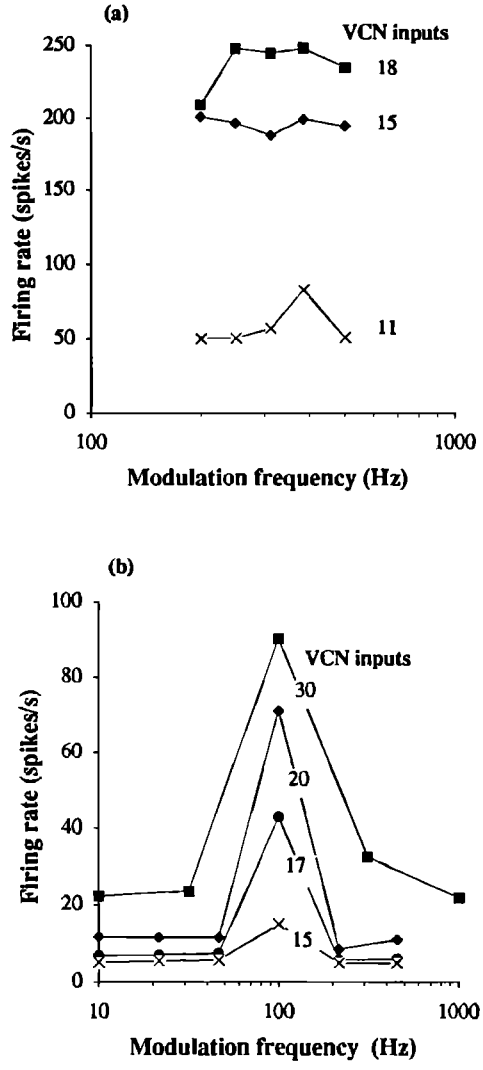

FIG. 16. Effect of changing the number of VCN chopper inputs to the model ICC unit. (a) A 400-Hz BMF unit which shows a bandpass rate-MTF with 11 model VCN chopper units becomes flat as the number of inputs increases. (b) A 100-Hz BMF unit which shows a bandpass rate-MTF with 30 model VCN chopper units remains bandpass as the number of inputs decreases.

Conversely, the effect of varying the number of VCN inputs to model units with low BMFs had a less marked influence. Figure 16(b) shows model rate-MTFs for an ICC unit with differing number of inputs. The BMF of the unit is 100 Hz. Although the peak firing rate decreases with smaller numbers of inputs, the bandpass nature of the functions is preserved in all cases.

These data allow us to speculate on an important issue raised in the literature. The issue concerns the ranges and distributions of BMFs in the VCN and ICC. Although the range of BMFs is similar for the VCN and ICC, the distribution of BMFs is shifted to *lower* AM frequencies in the ICC relative to the VCN (see Langner, 1992, Table I). The model provides us with a candidate explanation for this finding. Assume a population of model ICC units where the number of VCN inputs was drawn from a sample normally distributed around a mean number, for example 30. Given the data in Fig. 16 then we would expect to find only

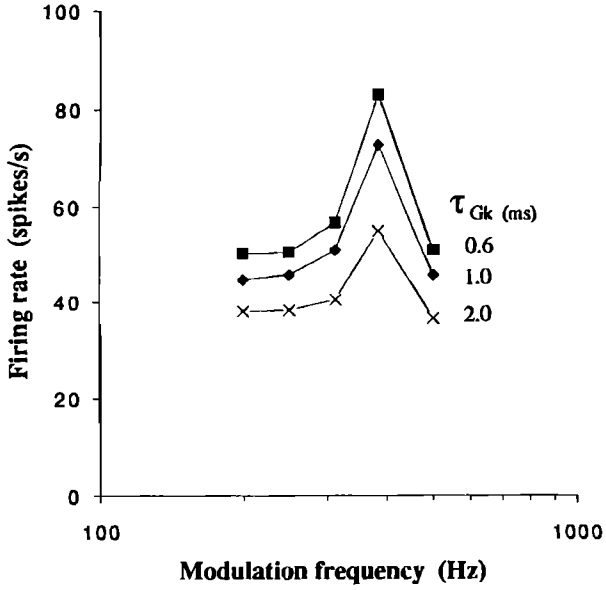

FIG. 17. Effect of changing τ_{Gk} on model ICC rate-MTFs.

a few model ICC units with high BMFs [because bandpass units with high BMFs only result with a small number of inputs, Fig. 16(a)], but many units with low BMFs [because bandpass units with low BMFs result both with a small number of inputs as well as with many inputs, Fig. 16(b)].

The post-spike recovery time is an important determinant of the response characteristics of the model VCN chopper cell used in this study. The recovery time is largely determined by the parameter τ_{Gk}. Figure 17 shows a typical result of changing τ_{Gk} on the model ICC unit. The example chosen shows a peak firing rate to a modulation frequency of 400 Hz. The effect of increasing τ_{Gk} is to decrease the rate of firing across the range of modulation frequencies, with the largest reduction in rate at 400-Hz modulation frequency. Thus it appears that τ_{Gk} simply limits the peak rate response of the ICC unit; it has no effect on the tuning of the unit to 400-Hz modulation frequency.

IV. DISCUSSION

We have described and evaluated a computer model of a neural circuit that can replicate the AM sensitivity of units within the auditory system at the level of the auditory nerve, the cochlear nucleus and inferior colliculus.

The main finding of this study is that a computer simulation of the neural circuit outlined in Fig. 2 can qualitatively replicate a number of complex response behaviors of cells in the auditory brain stem. The most striking example of this is seen in the rate modulation transfer functions of the ICC model (Fig. 10). In common with neural data, the model shows a peak of firing to a particular modulation frequency. The rate of firing, however, does not necessarily imply a particular rate of signal amplitude modulation. In fact, the rate of firing at a unit's preferred amplitude modulation frequency is a nonmonotonic function of signal level; first the firing rate increases with signal level reaching a maximum at about 20–30 dB above unit threshold, followed by a decrease in rate for increases in stimulus level thereafter.

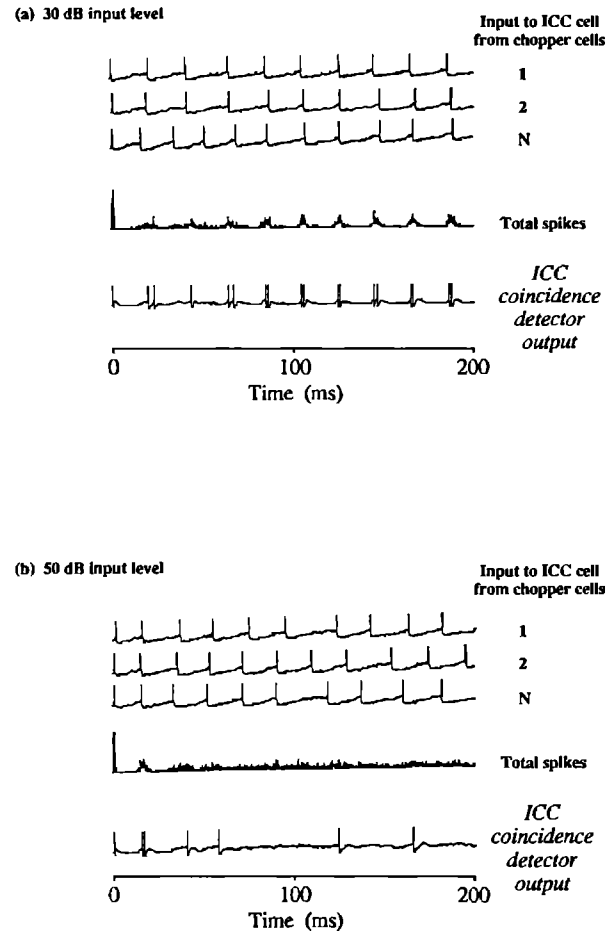

FIG. 18. Model output in response to a 50-Hz AM tone. (a) 30 dB above threshold. (b) 50 dB above threshold.

A. Mechanism

The responses of the cochlear nucleus chopper cells provide the basis of an explanation for this complex behavior. Frisina *et al.* (1990) found that certain units in the VCN showed bandpass temporal-MTFs for stimuli at moderate and high stimulus levels. They also noted that the peak modulation gain decreased with increases in stimulus level. The decrease in gain was on average 5 dB over a 20-dB range (i.e., 30–50 dB above threshold) but could be as high as 10 dB. The effect is replicated in the temporal-MTFs of the model chopper cell presented here (see Fig. 5). The reduction in modulation gain reflects a tendency for the output spikes to become more distributed across the positive half of the waveform envelope.

This effect can be observed in Fig. 18 which shows output from model chopper cells in response to AM stimuli presented at two different levels. At 30 dB above unit threshold, action potentials are only generated during a limited portion of the signal's modulation envelope, namely at the peak of the envelope. In contrast, at 50 dB above threshold action potentials are generated over a relatively wider portion of the signal's envelope. The rela-

tively wide distribution of spikes is due to two factors. First, a high signal level means that a greater portion of the signal's amplitude envelope is sufficiently high to produce action potentials from the cell. Second, the response at the peak of the amplitude envelope is limited by the cell's saturation threshold such that increases in stimulus level above the threshold do not engender further increases in spike rate. This means that as the stimulus level increases over moderate and high signal levels the spike rate remains relatively constant but the timing of the spikes relative to the modulation envelope changes.

In the model presented here, the spike trains from the cochlear nucleus cells form the input to the model ICC coincidence detector. In Fig. 18(a) the output spikes are highly coincidental because they are locked to the amplitude envelope of the same signal. Hence, the output rate of the model ICC unit will be relatively high. In Fig. 18(b) the output from the chopper cells occur relatively asynchronously, and there are less coincidences to drive the ICC unit. As the synchrony of spikes of the model VCN unit decreases with increases in stimulus level then so does the output rate of the coincidence detector (e.g., Fig. 10).

A complete explanation of the model ICC responses requires consideration of two factors. The first is the level-dependent change in the temporal output of the VCN unit and the second is the level-dependent change in overall spike rate of the VCN unit. In the first case the degree of synchrony decreases with increases in stimulus level (Fig. 5), and in the second case the firing rate increases with increases in stimulus level (not shown). For AM stimuli at peak modulation frequency the changes in synchrony appear to dominate the response of the ICC unit. That is, the firing rate of the ICC unit falls as the synchrony of the VCN unit falls. The influence of the rising VCN output rate is not apparent in the response of the ICC rate. At very low modulation frequencies and high modulation frequencies (e.g., 10 and 500 Hz) the situation is reversed. Here, the synchrony of the VCN unit falls with increasing level (down to less than −10-dB modulation gain) but the rate of the ICC unit increases with level. In this case the synchrony is too low to influence the response of the ICC unit and the response is dominated by the rise in VCN firing rate.

B. Anatomical and physiological basis of the model

It is useful to review the known anatomy and physiology upon which the model is based. First, it has been shown that axons of ventral cochlear nucleus chopper cells do project to the ICC (Roth *et al.*, 1978; Adams, 1979). Smith and Rhode (1989) examined the terminals of VCN chopper cell axon collaterals to find small round vesicles which are indicative of an excitatory synapse. Thus the evidence to date on VCN/ICC pathways does not contradict the existence of an ascending excitatory circuit between cells of the two nuclei. Alternatively, fusiform units from the dorsal CN (DCN) may provide the input to the ICC unit. Fusiform cell axons leave the DCN via the dorsal acoustic stria and terminate in the ICC and also have presumed excitatory endings (Ryugo and Willard, 1985; Smith and Rhode, 1985). These cells generally show a pauser/build-up type post-stimulus time histogram in response to pure tones presented at CF (Godfrey *et al.*, 1975; Rhode *et al.*, 1983; Smith and Rhode, 1985; Rhode and Smith, 1986). Kim *et al.* (1990) have shown that DCN/PVCN fusiform cells also show bandpass temporal-MTFs similar to those presented here from the model chopper cell. Onset cells in the VCN also show bandpass temporal-MTFs with high modulation gains (Frisina *et al.*, 1990).

To our knowledge there are no data concerning possible synaptic arrangements (i.e., number of inputs, dendritic or somatic input) between CN stellate (or fusiform) cells and ICC cells which may support the configuration we have proposed here. These remain predictions of the model. In addition, there are no relevant data on the membrane properties of ICC cells.

Langner (e.g., 1981; see Langner, 1992 for details and references) has proposed an alternative model which accounts for some of the response properties of ICC units in response to amplitude-modulated stimuli. The model was proposed to explain aspects of human pitch perception on the basis of verifiable physiological findings.

Langner's model, in common with the one presented here, is a coincidence model, but the inputs to the final coincidence detector unit arrive from two different sources and not one as proposed here. Moreover, the two inputs to the coincidence unit each require preprocessing by an additional circuit element before the input is directed to the ICC unit. The single source of input to the coincidence model presented here does not require any such preprocessing. The model proposed here benefits from its relative simplicity. However, Langner's model is more consistent with the gross architecture of the ICC where a single frequency/cochlear representation consists of converging afferent inputs from multiple brainstem sources (Irvine, 1986).

Other differences between the models concern the nature of implementation. The model presented here consists of realistic simulations of known neural elements that are present at the level of the auditory nerve, the cochlear nucleus and the inferior colliculus. In contrast, Langner's model is more phenomenologically based and uses elements such as trigger units, oscillators, reducer circuits and coincidence detection, although Langner has attempted to make correspondences between these elements and the properties of neurons located in the cochlear nucleus and inferior colliculus (Langner *et al.*, 1987).

Given these differences and intricacies of the models it is difficult to predict their behavior to novel stimuli without resorting to full-scale simulation. However, given that both models produce predictions which cannot be tested by reference to data already in the literature we may postpone detailed, full-scale evaluations for the time being. Ideally, future empirical investigations will address some of the predictions made by the models and will be able to provide evidence for the success or otherwise of each one.

TABLE AI. VCN chopper and ICC model parameters (ranges given in parentheses).

Parameter	Description	VCN chopper cell	ICC cell
Ek	Equilibrium potential for potassium	−10 mV	−10 mV
τ_m	Post-synaptic membrane time constant	(1–3 ms)	1.0 ms
τ_{Gk}	Potassium conductance time constant	(0.3–6 ms)	0.6 ms
b	Spike-induced potassium conductance	0.08	0.017
τ_{Th}	Threshold time constant	20 ms	20 ms
c	Voltage induced rate of threshold change	0.1	0.1
Th 0	Resting threshold	15 mV	20 mV

C. Modeling populations of units

Langner and Schreiner (1988; Schreiner and Langner, 1988) have presented data for the existence of a modulation map in the ICC. They propose that for each characteristic frequency there exists a secondary axis comprising neurons systematically arranged to encode perceptually relevant signal modulations. In the results presented here we have successfully modeled this arrangement at a single characteristic frequency. Future work will extend the model presented here to replicate the encoding of modulation at other characteristic frequencies as demonstrated neurally. The following issues will be addressed.

Hewitt *et al.* (1992) reported that the number of auditory nerve inputs to the VCN chopper unit influenced the shape of its temporal modulation transfer function; a small number of inputs (e.g., 5) gave rise to a lowpass transfer function while many inputs (e.g., 60) gave a sharply tuned bandpass function. As a consequence for the work reported here we modeled 60 auditory nerve inputs to each VCN chopper cell. All of the early testing of the model ICC unit was performed by modeling 60 VCN chopper inputs to each ICC cell. The best-modulation frequency of the VCN and ICC units was tuned to 50 Hz. Later, we noted that with higher best-modulation frequencies the functioning of the model ICC unit only continued in a manner consistent with the physiology if the number of VCN chopper inputs was reduced. A detailed examination of this behavior will be made.

A second issue concerns the upper limit of best-modulation frequencies. Rees and Møller (1983) reported that the most effective modulation rates in their sample of ICC units were between 20 and 40 Hz; none of the units responded to modulation frequencies greater than 80 Hz. Langner and Schreiner (1988) reported that 50% of their ICC recordings revealed best-modulation frequencies of between 30 and 100 Hz, but 20%–30% of units had BMFs greater than 100 Hz, some as high as 500 Hz. The discrepancy between the findings of Langner and Rees has been raised in the literature; levels of anaesthesia and sampling density have been proposed to account for the difference in the range of BMFs reported by the two studies.

In the model presented here we have produced a range of units with BMFs between 50 and 400 Hz. Langner and Schreiner (1988), however, also reported that the upper limit of ICC BMFs was dependent upon characteristic frequency. For a given CF below 4 kHz, no units were found that had BMFs above the quotient CF/4. Future work will address this issue using a multichannel (CF) version of the model presented above.

V. CONCLUSIONS

We have presented and evaluated a computer model of a neural circuit that replicates amplitude-modulation sensitivity of cells in the central nucleus of the inferior colliculus (ICC). The circuit we propose comprises an ICC unit which receives input from many cochlear nucleus chopper cells which, in turn, receive input from many auditory-nerve fibers. We speculate that the ICC unit functions as a coincidence detector taking input from a number of similar cochlear nucleus cells. The coincidence unit only fires when it receives a number of synchronous cochlear nucleus inputs. The circuit is sufficient to encode signal periodicity as a rate-based code.

ACKNOWLEDGMENTS

This research was supported by a grant from the Image Interpretation Initiative of the Science and Engineering Research Council, UK (GR/H/52634), a Basic Research grant from the Esprit programme of the European Community (BRA grant SSS 6961), and an equipment grant from Apple Computers Inc., USA. We thank the two anonymous reviewers who provided helpful comments on an earlier version of this paper.

APPENDIX

Point neuron model (MacGregor, 1987, p. 458).

The model is activated by a single input function which represents the stimulating current from an experimentally applied electrode. The model is characterized by four variables: (1) The transmembrane potential measured as a deviation from the cell resting potential; (2) a potassium conductance; (3) the time-varying threshold; and (4) an all-or-nothing spiking variable. Changes in these variables are governed by four differential equations. The first describes the change in the transmembrane potential in response to input current:

$$\frac{dE(t)}{dt} = (-E(t) + \{[I(t)/G] + Gk(t)/G[Ek - E(t)]\})/\tau_m, \quad \text{(A1)}$$

where $E(t)$ = instantaneous cell-membrane potential above resting level, E_R, $E(0)=0$, $G_k(t)$ = instantaneous cell potassium conductance. $G_k(0)=0$, G = total resting conductance of soma, τ_m = membrane time constant, E_k = equilibrium potential of potassium conductance relative to cell resting level, and $I(t)$ = current at the soma.

The equation describing the change in potassium conductance is as follows

$$\frac{dGk(t)}{dt}=\frac{[-Gk(t)+(b\cdot s)]}{\tau_{Gk}}, \tag{A2}$$

where b = delayed rectifier potassium conductance strength, s = spiking variable (0 or 1), $s=0$ if $E(t)<\mathrm{Th}(t)$, $s=1$ if $E(t)\geqslant\mathrm{Th}(t)$. τ_{Gk} = time constant of potassium conductance decay.

Here, Gk rises following an action potential but, otherwise, is continually reducing to zero. The model includes a term for accommodation whereby a cell's firing threshold varies as a function of stimulation. The equation describing the change in threshold is as follows

$$\frac{d\,\mathrm{Th}(t)}{dt}=\frac{\{-[\mathrm{Th}(t)-\mathrm{Th}\,0]+c\,E(t)\}}{\tau_{\mathrm{Th}}}, \tag{A3}$$

where $\mathrm{Th}(t)$ = time-varying threshold of the cell, $\mathrm{Th}\,0$ = resting threshold of the cell, c = accommodation constant, τ_{Th} = time constant of threshold.

The main output function, $p(t)$, is a combination of the transmembrane potential and the spiking variable and represents the record that would be measured with an intracellular microelectrode:

$$p(t)=E(t)+s[Eb-E(t)], \tag{A4}$$

where E_b = constant representing spike height (50 mV), s = spiking variable (see above). A spike is counted when $s=1$. See Table AI.

[1]Most of the early testing of the model used $\tau_m=3$ ms. Later, with $\tau_m=1$ ms a complete range of BMFs (50–400 Hz) could be generated by manipulation of a single model parameter, namely τ_{Gk}.

Adams, J. C. (1979). "Ascending projections to the inferior colliculus," J. Comp. Neurol. **183**, 519–538.

Aitkin, L. (1986). *The Auditory Midbrain* (Humana, Clifton, NJ).

Arle, J. E., and Kim, D. O. (1991). "Neural modeling of intrinsic and spike-discharge properties of cochlear nucleus neurons," Biol. Cyber. **64**, 273–283.

Assmann, P. F., and Summerfield, Q. (1989). "Modeling the perception of concurrent vowels: Vowels with the same fundamental frequency," J. Acoust. Soc. Am. **85**, 327–338.

Banks, M. I., and Sachs, M. B. (1991). "Regularity analysis in a compartmental model of chopper units in the anteroventral cochlear nucleus," J. Neurophysiol. **65**, 606–629.

Batra, R., Kuwada, S., and Standford, T. R. (1989). "Temporal coding of envelopes and their interaural delays in the inferior colliculus of the unanesthetized rabbit," J. Neurophysiol. **61**, 257–268.

Eggermont, J. J. (1991). "Rate and synchronization measures of periodicity coding in cat primary auditory cortex," Hear. Res. **56**, 153–167.

Frisina, R. D., Smith, R. L., and, Chamberlain, S. C. (1990). "Encoding of amplitude modulation in the gerbil cochlear nucleus: I. A hierarchy of enhancement," Hear. Res. **44**, 99–122.

Godfrey, D. A., Kiang, N. Y. S., and Norris, B. E. (1975). "Single unit activity in the dorsal cochlear nucleus of the cat," J. Comp. Neurol. **162**, 269–284.

Goldberg, J. M., and Brown, P. B. (1969). "Responses of binaural neurons of dog superior olivary complex to dichotic tonal stimulation: Some physiological mechanisms of sound localization," J. Neurophysiol. **32**, 940–958.

Ghoshal, S., Kim, D. O., and Northrop, R. B. (1992). "Amplitude-modulated tone encoding behavior of cochlear nucleus neurons: Modeling study," Hear. Res. **58**, 153–165.

Hastings, N. A. J., and Peacock, J. B. (1975). *Statistical Distributions* (Butterworths, London).

Hewitt, M. J., and Meddis, R. (1993). "Regularity of cochlear nucleus stellate cells: A computational modeling study," J. Acoust. Soc. Am. **93**, 3390–3399.

Hewitt, M. J., Meddis, R., and Shackleton, T. M. (1992). "A computer model of a cochlear nucleus cell: Responses to pure-tone and amplitude-modulated stimuli," J. Acoust. Soc. Am. **91**, 2096–2109.

Hodgkin, A. L., and Huxley, A. F. (1952). "A quantitative description of membrane current and its application to conduction and excitation in nerve," J. Physiol. (London) **117**, 500–544.

Irvine, D. R. F. (1986). *Progress in Sensory Physiology 7: The Auditory Brainstem* (Springer-Verlag, Berlin).

Javel, E. (1980). "Coding of AM tones in the chinchilla auditory nerve: Implications for the pitch of complex tones," J. Acoust. Soc. Am. **68**, 133–146.

Joris, P. X., and Yin, T. C. T. (1992). "Responses to amplitude-modulated tones in the auditory nerve of the cat," J. Acoust. Soc. Am. **91**, 215–232.

Khanna, S. M., and Teich, M. C. (1989). "Spectral characteristics of the responses of primary auditory-nerve fibers to amplitude-modulated signals," Hear. Res. **39**, 143–158.

Kim, D. O., Sirianni, J. G., and Chang, S. O. (1990). "Responses of DCN-PVCN neurons and auditory nerve fibers in unanaesthetized decerebrate cats to AM and pure tones: Analysis with autocorrelation/power-spectrum," Hear. Res. **45**, 95–113.

Langner, G. (1981). "Neuronal mechanisms for pitch analysis in the time domain," Exp. Brain Res. **44**, 450–454.

Langner, G. (1992). "Periodicity coding in the auditory system," Hear. Res. **60**, 115–142.

Langner, G. Decker, J., Günther, M., and Hose, B. (1987). "A computer model for periodicity analysis in the auditory midbrain based on physiological properties and connectivities of units in the cochlear nucleus," Soc. Neurosci. Abstr. **13/1**, 546.

Langner, G., and Schreiner, C. E. (1988). "Periodicity coding in the inferior colliculus of the cat: I. Neuronal mechanisms," J. Neurophysiol. **60**, 1799–1822.

Lesser, H. D., O'Neill, W. E., Frisina, R. D., and Emerson, R. G. (1990). "On-off units in the moustached bat inferior colliculus are selective for transients resembling acoustic glint from fluttering insect targets," Exp. Brain Res. **82**, 137–148.

MacGregor, R. J. (1987). *Neural and Brain Modeling* (Academic, San Diego, CA).

Meddis, R. (1986). "Simulation of mechanical to neural transduction in the auditory receptor," J. Acoust. Soc. Am. **79**, 702–711.

Meddis, R. (1988). "Simulation of auditory-neural transduction: Further studies," J. Acoust. Soc. Am. **83**, 1056–1063.

Meddis, R., and Hewitt, M. J. (1991). "Virtual pitch and phase sensitivity of a computer model of the auditory periphery: I. Pitch identification," J. Acoust. Soc. Am. **89**, 2866–2882.

Meddis, R., Hewitt, M. J., and Shackleton, T. M. (1990). "Implementation details of a computational model of the inner hair-cell/auditory-nerve synapse," J. Acoust. Soc. Am. **87**, 1813–1816.

Møller, A. R. (1972). "Coding of amplitude and frequency modulated sounds in the cochlear nucleus of the rat," Acta Physiol. Scand. **86**, 223–238.

Møller, A. R. (1973). "Statistical evaluation of the dynamic properties of cochlear nucleus units using stimuli modulated with pseudo-random noise," Brain Res. **57**, 443–456.

Møller, A. R. (1976). "Dynamic properties of primary auditory fibers compared with cells in the cochlear nucleus," Acta Physiol. Scand. **98**, 157–167.

Müller-Preuss, P. Bieser, A., Preuss, A., and Fastl, H. (1988). "Neural processing of AM sounds within the central auditory pathway," in *Auditory Pathway: Structure and Function*, edited by J. Syka and R. B. Masterton (Plenum, New York), pp. 327–331.

Oertel, D. (1985). "Use of brain slices in the study of the auditory sys-

tem: spatial and temporal summation of synaptic inputs in cells in the anteroventral cochlear nucleus of the mouse," J. Acoust. Soc. Am. **78**, 328–333.

Oertel, D., Wu, S. H., and Hirsch, J. A. (**1988**). "Electrical characteristics of cells and neuronal circuitry in the cochlear nuclei studied with intracellular recordings from brain slices," in *Auditory Function*, edited by G. M. Edelman, W. E. Gall, and W. M. Cowan (Wiley, New York), pp. 313-336.

Palmer, A. R. (**1982**). "Encoding of rapid amplitude fluctuations by cochlear nerve fibers in the guinea pig," Arch. Otorhinolaryngol. **236**, 197–202.

Patterson, R. D., Nimmo-Smith, I., Holdsworth, J., and Rice, P. (**1988**). "Spiral vos final report, Part A: The auditory filterbank," Cambridge Electronic Design. Contract Rep. (APU 2341).

Rees, A., and Møller, A. R. (**1983**). "Responses of neurons in the inferior colliculus of the rat to AM and FM tones," Hear. Res. **10**, 301–330.

Rees, A., and Møller, A. R. (**1987**). "Stimulus properties influencing the responses of inferior colliculus neurons to amplitude-modulated sounds," Hear. Res. **27**, 129–143.

Rees, A., and Palmer, A. R. (**1989**). "Neuronal responses to amplitude-modulated and pure-tone stimuli in the guinea pig inferior colliculus, and their modification by broadband noise," J. Acoust. Soc. Am. **85**, 1978–1994.

Rhode, W. S., and Smith, P. H. (**1986**). "Physiological studies on neurons in the dorsal cochlear nucleus of the cat," J. Neurophysiol. **56**, 287–307.

Rhode, W. S., Smith, P. H., and Oertel, D. (**1983**). "Physiological response properties of cells labeled intracellularly with horseradish peroxidase in cat dorsal cochlear nucleus," J. Comp. Neurol. **213**, 426–447.

Roth, G. L., Aitkin, L. M., Andersen, R. A., and Merzenich, M. M. (**1978**). "Some features of the spatial organization of the central nucleus of the inferior colliculus of the cat," J. Comp. Neurol. **182**, 661–680.

Ryugo, D. K., and Willard, F. H. (**1985**). "The dorsal cochlear nucleus of the mouse: a light microscope analysis of neurons that project to the inferior colliculus," J. Comp. Neurol. **242**, 381–396.

Schreiner, C. E., and Langner, G. (**1988**). "Periodicity coding in the inferior colliculus of the cat: II. Topographical organization," J. Neurophysiol. **60**, 1823–1840.

Smith, P. H., and Rhode, W. S. (**1985**). "Electron microscope features of physiologically characterized, HRP-labelled fusiform cells in the cat dorsal cochlear nucleus," J. Comp. Neurol. **237**, 127–143.

Smith, P. H., and Rhode, W. S. (**1989**). "Structural and functional properties distinguish two types of multipolar cells in the ventral cochlear nucleus," J. Comp. Neurol. **282**, 595–616.